Saudi Pharmaceutical Journal 30 (2022) 532–543

Contents lists available at ScienceDirect

Saudi Pharmaceutical Journal

journal homepage: www.sciencedirect.com

Original article

Study on chemical constituents of Folium *Artemisiae argyi* Carbonisatum, toxicity evaluation on zebrafish and intestinal hemostasis

Le Gu, Xueyu Wang, Xinting Shao, Yuling Ding *, Yong Li *

School of Pharmaceutical Sciences, Changchun University of Chinese Medicine, Changchun 130117, Jilin, China

ARTICLE INFO

Article history:
Received 9 January 2022
Accepted 27 February 2022
Available online 2 March 2022

Keywords:
Folium *Artemisiae argyi* Carbonisatum
Chemical composition
Zebrafish
Toxicity
Hemostasis

ABSTRACT

Folium *Artemisiae argyi* Carbonisatum (FAAC) is a traditional medicine widely used in clinic. It has the effect of hemostasis by warming meridians. In order to further explore the chemical composition and biological activity of FAAC, the methanol extract of FAAC was isolated and purified by open column and high-performance liquid chromatography. and the complete structure was characterized by nuclear magnetic resonance (NMR) and LREI-MS for the first time, namely rutin, quercetin and octacosanol respectively. Initially the toxic effect of methanol extract of FAAC on zebrafish was evaluated by observing the phenotypic characteristics, spontaneous twitch times, heart rate, hatching rate, the distance of SV-BA and cardiomyocyte apoptosis of zebrafish. The results showed that FAAC has embryonic development toxicity and cardiotoxicity when it was higher than 62.5 μg/mL. Meanwhile, the hemostatic effect of methanol extract of FAAC was compared with FAA (Folium *Artemisia argyi*) by zebrafish intestinal bleeding model originally. The results showed that the hemostatic effect of the medium and high concentration dose groups (3.0 and 30.0 μg/mL) was enhanced for both FAAC and FAA. This study provided an experimental basis for the clinical application of FAAC.

1. Introduction

FAA is the dry leaf of *Artemisia argyi* Lévl.et Vant, a perennial herb in the composite family. It is widely used as food and herbal medicine. As being a Traditional Chinese Medicine (TCM), FAA can stop bleeding, dispel cold and relieve pain. It contains a variety of chemical components such as volatile oil, flavonoids, tannins and triterpenoids (Song and Wen, 2019; Cui et al., 2020; Zhang et al., 2019). It has many pharmacological activities like antibacteria and antivirus (Guan et al., 2019), antiasthmatic, antitussive and expectorant, liver protection, antitumor (Seo et al., 2003) and antioxidant (Xia et al., 2019; Xiao et al., 2019). After high-temperature combustion, FAA turns into a charcoal herb, named Folium *Artemisiae Argyi* Carbonisata (FAAC) in TCM. FAAC is used to treat irregular menstruation, infertility, hematemesis, and diseases due to cold. It has also been reported that the carbon dots in FAAC can enhance the frost resistance (Kong et al., 2021). According to the theory of maintaining medicinal properties after the carbonisatus, the process of high-temperature charcoal frying of FAA is carbonization rather than ashing. Volatile components such as eucalyptol volatilize, but some non-carbonized organic compounds were remained with new generating substances. At present, there are many reports on the chemical components and pharmacological effects of FAA (Chen et al., 2017a; Lee et al., 2018; Zhang et al., 2013a), but the research on the chemistry, toxicity evaluation and bioactivity of FAAC is very rare. Therefore, it is particularly urgent to study the chemical composition of FAAC. In addition, based on the TCM theories such as "Charcoal frying to stop bleeding", "Black can overcome red, and bleeding will be stopped when black is seen", the hemostatic effect of FAA after charcoal frying is significantly enhanced, which is not only related to the formation of carbon or the significant reduction of insoluble calcium oxalate clusters and the production of free calcium ions, but also closely related to the reduction of NO and tissue factor pathway inhibitor (TFPI) content, and the increase of von Willebrand factor (vWF) content. Therefore, the hemostatic mechanism of FAAC needs to be further studied. The literatures show that quercetin (flavonoids) promotes blood coagulation by shortening activated partial thromboplastin time (APTT) and increasing fibrinogen (Chen et al., 2019a). Rutin (flavone glycosides) is often

* Corresponding authors.
E-mail addresses: dingyl@ccucm.edu.cn (Y. Ding), liyong@ccucm.edu.cn (Y. Li).
Peer review under responsibility of King Saud University.

Production and hosting by Elsevier

https://doi.org/10.1016/j.jsps.2022.02.018
1319-0164/

combined with vitamin C to form new medication (compound rutin tablets), and then to shrink uterine smooth muscle and inhibit postpartum hemorrhage in women by reducing vascular permeability and brittleness and reducing NO production (Li, 2021). In fact, the saponins and quercetin in Panax notoginseng have a two-way regulatory effect on the coagulation system under different dosage, so that Panax notoginseng can prevent bleeding and coagulation at the same time (Wang et al., 2008). Therefore, the non-carbonized flavonoids in FAAC provide a theoretical basis for the enhancement of hemostasis after carbonization.

In this paper, zebrafish model was selected for the first time to evaluate the toxicity and hemostatic effect of FAAC. The model system is a tropical teleost fish from the family Cyprinidae, originating from the Ganges River system, Burma, the Malakka peninsula, and Sumatra. Zebrafish can adapt to environmental factors such as temperature and pH value, and can grow for about 3 months in a short time at a water temperature of 26 ℃. It has the advantages of low feeding cost, small size, short development cycle, in vitro fertilization, transparency and easy observation, and high number of eggs per time. It is easy to realize high-throughput screening. At present, it has been widely used in the screening of active substances of TCM with complex chemicals (Adrià et al., 2020; Benchoula et al., 2019; Kang et al., 2018; Sheel et al., 2020). In addition, zebrafish can solve the problems of maintenance cost and life cycle time of conventional model animals. Its transparent body are convenient to detect the toxic effects of substances, such as teratogenicity, lethality and reproductive toxicity. Due to the genetic and physiological similarities with mammals, zebrafish is often used on toxicity screening models of drugs, chemicals, genes, xenobiology and nanomaterials, etc. (Makkar et al., 2018; Verma et al., 2021b).

As a processing of Chinese materia medica widely used in clinic, the biological activity and toxicological evaluation on FAAC were particularly important. However, its toxicological research has not been reported. In order to better ensure the drug safety, it can be assumed that the analysis of FAAC extract can not only explain that the process of high-temperature charcoal frying of FAA is carbonization rather than ashing, but also determine the safe and effective extraction process through activity and toxicity evaluation and analysis. In this study, the methanol extract of FAAC was used to evaluate the hemostatic effect on zebrafish toxicity and intestinal bleeding model. The chemical components of methanol extract were characterized by NMR and MS to evaluate zebrafish embryonic development and cardiotoxicity, so as to determine the best safe concentration of FAAC. The hemostatic effect of FAAC was evaluated by comparing the intestinal bleeding rate of zebrafish between FAA and FAAC. The purpose was to lay a solid foundation for the clinical application safety of processing of Chinese materia medica, and provide a basis for revealing the theory of maintaining medicinal properties after the carbonisatus.

2. Materials and methods

2.1. Instrument and materials

^{1}H NMR (400 & 600 MHz) and ^{13}C NMR (100 & 150 MHz) spectra were recorded on the AVANCE spectrometer (AVANCE™ III-400 & 600 NMR, Bruker BioSpin, Germany), using DMSO d_6 and $CDCl_3$ solvent as NMR regents, and an internal reference standard (tetramethylsilane, TMS). LREI-MS (Quattro Premier XE, Waters Co., Ltd, America, Ionization Mode:ESI+/-, Function Type:Full Scan, Capillary:3.0 kV/2.9 kV, Cone:20 V, Source Temperature:110 ℃, Cone Gas Flow:N_2, 80 L/Hr, Desolvation Temperature:480℃, Desolvation Gas Flow:N_2, 600 L/Hr). Silica gel column chromatography (200–300 mesh, Qingdao Marine Chemical Co., Ltd., China) and high-performance liquid chromatography (HPLC) were used for separation and purification, (Waters: 600 controller, delta 600, 2487, America; Agilent: 1260 Infinity II, America) and the chromatographic column (GS-120–5-SIL, 10 mm × 250 mm, GSA10250SIL19001, China Global chromatography Co., Ltd.; SHIMADZU C18 10 mm × 250 mm). The reagents used in HPLC were chromatographic pure, and other reagents were analytical pure. Ultraviolet–Visible Spectrophotometer (SB16-752, Beijing Zhongxi Yuanda Technology Co., Ltd, China) was used to determine the content of total flavonoids in ACCF. Zebrafish images were recorded by Olympus Fluorescence Inverted Microscope (IX73, Olympus TH4-200, Olympus U-RFL-T, Olympus, Japan), DMSO (1121e03210, ≥ 99.9%, Solarbio Biotechnology Co., Ltd., China) was used as a solvent for *in vivo* activity experiment, and the working concentration never exceeded 0.2% (v/v). FAA was purchased from Qichun of Hubei (Hongzhong Pharmaceutical Co., Ltd., China). It was identified by Professor Zhang Jinglong, School of Pharmaceutical Sciences, Changchun University of Chinese Medicine as *Artemisi argyi* Lévl.etVant. FAAC was self-made in the laboratory. Cleaned the prepared pieces of FAA and removed the impurities, stems and ash chips before kneading and dispersing them in the cylindrical type stir-frying machines. Then set the bottom temperature of the pot at 180 ℃ and the rotating speed at 20 r/min. Took a small amount of water to spray evenly when the yellow smoking comes from the fried FAA. Stirred-fry for about 16 min until the surface of FAA was scorched black, fried dry and put out the fire star. Finally, took them out and cool them to obtain FAAC. Its appearance was irregular curly mass, and surface was dark brown, which was met the standard of FAAC in"Jilin Province Code for Processing of Traditional Chinese Medicine, China" (Jilin Medical Products Administration,2020). Rutin (3:100080–200707, 99.8%, China Institute for the control of pharmaceutical and biological products) was used to determine the content of total flavonoids. Simvastatin (RO5D11T133391, 97%, Yuanye Biotechnology Co., Ltd., China) was an inducer of intestinal bleeding in zebrafish juvenile. O-anisidine was employed (97%, 20210510, Shanghai Hongshun Biotechnology Co., Ltd., China) to stained zebrafish hemoglobin. The aqueous solution with the 0.01% (v/v) methylene blue (Electrophoretic grade, Tianjin Institute of photovoltaic fine chemistry, China) was applied to clean zebrafish embryos as a disinfectant. PBS (pH = 7.4, Beit Haemek Ltd., Israel) was used to dissolve acridine orange (AO, S19094, Yuanye Biotechnology Co., Ltd., China) and clean embryos. Zebrafish embryos survived in 12&24 well-plates (Corning company, USA). Wild type AB zebrafish was purchased from China Zebrafish Resource Center. Artemia was purchased from Tianjin Fengnian aquaculture Co., Ltd., China.

2.2. Chemical research

2.2.1. Determination of total flavonoids

Took about 25 mg of rutin and weighed accurately, put it into a 25 mL volumetric flask and added an appropriate amount of methanol. Then put it on a water bath to dissolve, added methanol to dilute to the scale after cool, shook well, accurately measured 20 mL, put it into a 100 mL volumetric flask, added water to the scale, shook well, and prepared a solution containing 0.2 mg rutin per 1 mL as the positive control solution.

Took about 0.5 g of the nine batches of FAAC powder, accurately weighed and placed them in 100 mL round bottom flasks respectively. Accurately added 50 mL of methanol, shook well and weighed, and then refluxed for 1 h, weighed again after cooling, made up the lost weight with methanol, shook well, and filtered, discarded the primary filtrate. Then took the continuous filtrate as the test solution.

Accurately weighed 1 mL, 2 mL, 3 mL, 4 mL, 5 mL, and 6 mL of the positive control solution described above, placed them in 25 mL volumetric flask respectively, added water to 6 mL, added

1 mL of 5% sodium nitrite solution, mixed well and placed for 6 min. Then added 1 mL of 10% aluminum nitrate solution, shook well, placed for 6 min followed by adding 10 mL of sodium hydroxide solution, added water to the scale, shook well, placed for 15 min, and then took the corresponding reagent as blank control based on the method mentioned here. The absorbance was measured at 511 nm wavelength by UV–vis spectrophotometry. The standard curve was drawn with absorbance as the ordinate and concentration as the abscissa.

Accurately sucked 3 mL of the test solution into a 25 mL volumetric flask. According to the method under the preparation of the standard curve, to measure the absorbance, recorded the weight of rutin in the test solution based on the standard curve, and calculated the total flavone content.

The systematic and accidental error were mainly investigated in the determination of total flavone by UV–vis spectrophotometry after precision, stability, repeatability and recovery test.

2.2.2. Study on chemical composition

1.0 kg of FAAC was extracted by reflux extraction with methanol for twice, and each time for 30 min (100 mL methanol was added per 8.0 g). The extract was concentrated to obtain 20.10 g crude extract. It was subjected to silica gel column chromatography and eluted with *n*-hexane/ethyl acetate in gradient steps (10:0–0:10) to give Fr.1–5. Fr.1 was purified by semi-preparative normal-phase HPLC (*n*-hexane/ethyl acetate = 10:1, 2.0 mL/min,365 nm), and to collect the eluent at Rt 35.7 min, the compound **3** (68.72 mg) was obtained after recrystallization. Fr.4 was purified by semi-preparative reverse-phase HPLC (acetonitrile/0.1% phosphoric acid = 55:45, 2.0 mL/min, 365 nm) to give compound **1** (63.10 mg, Rt 15.8 min) and **2** (75.69 mg, Rt 22.4 min).

2.3. Zebrafish feeding and maintenance

AB strain zebrafish were raised in a fully closed circulation system, bred and reproduced refer to the China Zebrafish Resource Center guide. Adult AB zebrafish were maintained under the common condition (a 14/10 h light/dark cycle, 28.5 ℃, pH:7.2–7.5, 550 μs/m). The newly hatched eggs of artemia were administrated twice a day at 9:00 and 17:30. At 20:00 before spawning, healthy and mature zebrafish were selected and placed in the incubator at the ratio of 2:1 in males and females. At 9:00 on the second day, the baffle of the incubator was pulled out and zebrafish were stimulated by light. After the completion of spawning, the dead and impurities were removed, the embryos were collected, washed, and disinfected with 0.01% (V/V) methylene blue solution, and cultured in a light incubator at 28.5 ℃. (Chen et al., 2017b; Zhang et al., 2018). All experiments were performed in accordance with the relevant animal practice guidelines and regulations of Changchun University of Chinese Medicine.

2.4. Study on embryotoxicity of zebrafish

The embryo toxicity test was conducted according to the method in the literature (Qian et al., 2018). Healthy 4 h post-fertilization (hpf) embryos (transparent fertilized eggs) were randomly transferred to different concentrations of methanol extract of FAAC (62.5, 125, 250, 500 and 1000 μg/mL) in the sterile 12 well plate. Each group was provided with 60 embryos (repeated experiment, n = 3). Change the sample solution once every 24 h and remove the dead embryos to ensure the stability of various parameters in the solution.

2.4.1. Observation of zebrafish embryonic development phenotype

Took the embryos developed in the culture medium as the blank control group, the development and morphological changes of embryos after drug exposure were observed, photographed and recorded by inverted optical microscope at 24, 48, and 72 hpf. The development and morphological changes of embryos were focused mainly on the length, deformity and organ abnormalities at each time point and the changes of the indexes above with the extension of exposure time.

2.4.2. Determination of spontaneous twitch, heart rate, and hatching rate of zebrafish embryos

Took the embryos developed in the culture medium as the blank control group, the number of spontaneous twitches of embryos within 1 min at 24 hpf, heart beats within 30 s at 48 and 72 hpf and the hatching rate of embryos at 72 and 96 hpf at each concentration were observed by inverted optical microscope. The changes of the above indexes were recorded with the extension of exposure time.

2.5. Zebrafish cardiotoxicity study

Healthy two days post fertilization (dpf) embryos were randomly transferred into different concentrations of methanol extract of FAAC (62.5, 125, 250, 500 and 1000 μg/mL) in the sterile 12 well-plate, 30 embryos in each group, and 10 embryos were taken for statistics (thrice). The changes of cardiac indexes were observed at 24, 48 and 72 h after administration. The sample solution of methanol extract of FAAC was changed every 24 h and the dead embryos were removed to ensure the stability of various parameters in the solution.

2.5.1. Observation of zebrafish embryonic heart development phenotype, heart rate and SV-BA

Zebrafish treated for 24 h, 48 h, and 72 h for each group were taken out from the constant temperature incubator, placed at room temperature for about 15 min, and then photographed and observed under the microscope. The changes of heart morphology and heart beat times of zebrafish (3 times per zebrafish) within 30 s at each time point were mainly recorded. At the same time, according to the photo scale, the actual length of sinus venous-bulbous arteriosus (SV-BA) was calculated by Image-Pro 7.0 analysis software.

2.5.2. Detection of cardiomyocyte apoptosis

The cardiomyocyte apoptosis was detected by AO staining (Elfawy et al., 2021; Zhu et al., 2015). Zebrafish embryos treated to 48 h after administration in each group were taken, the test solution of methanol extract of FAAC was removed, washed with culture water for 3 times, and then zebrafish embryos were stained with AO dye at 7.0 μg/mL in the dark for 30 min, and then washed twice with phosphate buffer (PBS, pH 7.4) (Patel et al., 2020; Verma et al., 2021a). After staining, the zebrafish embryos were placed in double concave slides, adjusted to the lateral decubitus position, and observed under a fluorescence microscope, calculated by Image-Pro 7.0 analysis software.

2.6. Evaluation of intestinal hemostasis in zebrafish

2.6.1. Half lethal dose (LD_{50}) test

The wild-type AB zebrafish at 2dpf were randomly selected and placed in 12 well-plates (30 embryos per well, capacity:3 mL n = 3). The blank control group under normal feeding and the six test groups of methanol extract of FAAC (62.5, 125, 250, 500, 1000 and 2000 μg/mL) were set up. The death of zebrafish was observed and recorded. Finally, the mortality of zebrafish in each group was counted to obtain the LD_{50}.

2.6.2. Establishment of zebrafish intestinal bleeding model

5dpf AB strain zebrafish were selected for the intestinal bleeding model based on the growth law of the first intestinal contraction at 4 dpf and eating at 5 dpf. Zebrafish (30 embryos per well, capacity:3 mL, n = 3) were randomly selected and placed in different concentrations (0,1, 2, 4, 6 and 8 μM). The induction time was set to 24 h. *O*-anisidine (containing 0.6 mg/mL *o*-anisidine, 0.01 M sodium acetate, 0.65% H_2O_2, 40% ethanol, dark staining for 30 min) was used to observe and record whether the model was successful under the microscope. The formula for calculating the incidence of intestinal bleeding in zebrafish: Incidence of bleeding (%) = (number of zebrafish with intestinal bleeding / number of the total) × 100%.

2.6.3. Calculation of intestinal bleeding rate

5dpf AB zebrafish were placed in 12 well plates (30 embryos per well, capacity:3mL, n = 3) and treated with different concentrations of methanol extract of FAA and FAAC (0.3, 3.0 and 30.0 μg/mL). At the same time, the blank and model control groups were set up. Simvastatin of 4.0 μM was used as the inducer. After 24 h the number of zebrafish with intestinal bleeding in each experimental group was observed and recorded under a microscope, and the efficacy of methanol extract of FAA and FAAC in reducing the incidence of intestinal bleeding was evaluated with the incidence of bleeding as statistical values.

2.7. Statistical methods

The data was statistically analyzed by Fisher's exact test and Dunnetťs test ($p < 0.05$ means significant difference, and $p < 0.01$ means extremely significant difference).

3. Results

3.1. Chemical research

3.1.1. Total flavonoids content

Rutin used as reference substance has the maximum absorption at 511 nm. The regression equation of standard curve was Y = 12.418x-0.0127, r = 0.999, there was a good linear relationship between rutin concentration and absorbance within the range of 0.0148 ∼ 0.0518 mM. The relative standard deviation (RSD) was recorded for the precision (0.04%), repeatability (0.18%), stability (0.06%) and recovery tests (0.94%). The content of total flavonoids in different nine batches of FAAC was among 5.9501 ∼ 7.0089% shown in Table 1.

3.1.2. Study on chemical composition

Three compounds were isolated from FAAC named as rutin (**1**), quercetin (**2**) and octacosanol (**3**), see Fig. 1, and the HMBC and TOCSY correlation spectra of compound **1** was shown Fig. 2.

The compound **1** is a light yellowish crystalline powder. According to LR-EIMS (*m*/*z*, 610.57), ^{1}H, ^{13}C and DEPT (distortionless enhancement by polarization transfer), the molecular formula of **1** is $C_{27}H_{30}O_{16}$ with thirteen unsaturation degree, which is composed of five rings and eight double bonds. The molecular structure of it is confirmed by 1D & 2D NMR comprehensive analysis. The ^{1}H NMR spectrum shows five aromatic proton signals, in which two protons at 6.39(1H, d, *J* = 2.1 Hz) and 6.20(1H, d, *J* = 2.1 Hz) coupled with each other (*J* = 2.1 Hz) indicate that the two protons are in the interphase position in the aromatic **A** ring, the other three protons at 7.54 (1H, d, *J* = 2.3 Hz), 6.85 (1H, d, *J* = 8.2 Hz) and 7.56 (1H, dd, *J* = 2.3 Hz, 8.2 Hz) construct a ABX advanced coupling system, which is elucidated in the aromatic **B** ring. The two hydrogen atoms at 5.34 (1H, d, *J* = 7.4 Hz) and 4.39 (1H, m) were assigned to terminal protons from the moieties of glucose and rhamnose, the signals at 3.20 ∼ 3.32 (1H, m), 3.71 (1H, d, *J* = 10.1 Hz) and 1.00 (3H, d, *J* = 6.2 Hz) are from –CH_2OH of glucose, and –CH_3 of rhamnose based on the chemical shift values and coupling constants, respectively. The three multiples at 3.04 ∼ 3.10 (1H, m), 3.20 ∼ 3.32 (5H, m) and 3.34 ∼ 3.42 (2H, m) belong to the other H signals on glucose and rhamnose. The ^{13}C and ^{13}C DEPT spectra show twenty-seven carbon atoms, including one CH_3, one CH_2, fifteen CH and ten C signals. Combined with HSQC (heteronuclear single quantum coherence) spectrum, the C-H structural units of it are conformed leading to preliminarily determination for flavonol glycoside. As to the linkage between the aglycone and sugars as well as the active hydrogens in it, are assessed mainly based on 2D ^{1}H–^{13}C HMBC (heteronuclear multiple bond connectivity) and ^{1}H–^{1}H NOESY (nuclear overhauser effect spectroscopy) in spectra. HMBC mainly reveals the interconnection of some structures, between HO-5 (δ_H: 12.60) on **A** ring and C-4 (δ_C: 177.8) in **C** ring, between H-2′, 6́ (δ_H:7.54 & 7.56) in **B** ring and C-2 (δ_C: 157.1) in C-ring, the connection between sugars and aglycon is set from the strong heteronuclear correlation because of H-1″ (δ_H: 5.34) to C-3 (δ_C: 133.8), and the linkage between rhamnose and glucose supported from the correlation of H-1″ (δ_H: 5.34) to C-6″ (δ_C: 67.5). Meanwhile, the relative configuration between glucose and aglycon was determined as β according to the 7.4 Hz coupling constant of terminal protons on glucose, H-1″ (δ_H: 5.34) to 2H-6″ (δ_H: 3.20 ∼ 3.32, 3.71) in NOESY spectrum, where indicate that the terminal –OH group was on the same side with the upward –CH_2OH, so the absolute configuration of glucose is D. The relation of H-1‴(δ_H: 4.39) to H-5‴(δ_H: 3.20 ∼ 3.32) has no appearance in the NOESY spectrum, however, the H-1‴ is related to the proton on terminal –CH_3, so the relative configuration of rhamnose is α, and the –CH_3 was under the ring, so rhamnose is α-L-type. In this structure, there are four phenolic hydroxyl groups on the flavanone, and their attribution is based on the HMBC spectrum, the 12.60 (1H, s) is coupled with C-5, 6 and 10, so the –OH belongs to C-5, compare with other phenolic hydroxyl protons, this –OH is located in the low field because it forms an intramolecular hydrogen bond with the ketone group at C-4 position. Although the other three phenolic hydroxyl protons show no correlation with C-5 and C-3′ & 4′ protons in **A** and **B** ring, the NOESY spectrum provides evidence with strong correlation between 10.81 (1H, s) and H-6 & 8, between 9.66 (1H, s) and H-2′, and between 9.16 (1H, s) and H-5′, finally the 10.81 signal is determined at HO-7, 9.66 at HO-3′, and 9.16 at HO-4′, respectively. The –OH protons on sugars are elucidated mainly based on HMBC spectrum, in which there were three free –OH on glucose, namely 5.28 at C-2″ to C-1″, 2″, 3″; 5.10 at C -3″ to C-2″, 3″, and 5.07 at C-4″ to C-4″, respectively. In the case of rhamnose, the strong correlation between 4.34 at C-2‴ and C-1‴, a weak correlation between 4.52 at C-3‴ and C-1‴, the other –OH is conformed in the range of 4.45 ∼ 4.36 (2H, m), of which one H belongs to rhamnose terminal proton, while the other H had no any correlation in HMBC, it only can be assigned to C-4‴. The TOCSY (total correlation spectroscopy) spectrum further confirms the attribution of hydrocarbon atoms on the two sugars. Compared with the literature, the compound **1** was identified as flavanol glycoside, namely rutin (Panida et al., 2020).

Compound **1:** yellow powder. LR-EIMS: *m*/*z*, 610.57 ($C_{27}H_{30}O_{16}$). ^{1}H NMR (600 MHz, DMSO d_6, TMS), δ_H: 6.20 (1H, d, *J* = 2.1 Hz, H-6), 6.39 (1H, d, *J* = 2.1 Hz, H-8), 7.54 (1H, d, *J* = 2.3 Hz, H-2′), 6.85 (1H, d, *J* = 8.2 Hz, H-5′), 7.56 (1H, dd, *J* = 2.3 Hz, 8.2 Hz, H-6′), 12.61 (1H, s, HO-5), 10.81 (1H, s, HO-7), 9.66 (1H, s, HO-3′), 9.16 (1H, s, HO-4′), 5.34 (1H, d, *J* = 7.4 Hz, H-1″), 3.20 ∼ 3.32 (6H, m, H-2″, 3″, 4″, 6″, 2‴, 5‴), 3.34 ∼ 3.42 (2H, m, H-5″, 3‴), 3.71 (1H, d, *J* = 10.1 Hz, H-6″), 5.28 (1H, d, *J* = 4.1 Hz, HO-2″), 5.10 (1H, d, *J* = 4.0 Hz, HO-3″), 5.07 (1H, d, *J* = 5.8 Hz, HO-4″), 4.39 (1H, m, H-1‴), 3.04 ∼ 3.10 (1H, m, H-4‴), 1.00 (3H, d, *J* = 6.2 Hz, H-6‴), 4.34

Table 1
Determination of total flavonoids in FAAC.

Batch*	Sample (g)	Absorbance value	Concentration (mg/mL)	Flavone content (mg)	Content (%)	Average (%)
A1	0.5001	0.6923	0.2975	29.7504	5.9501	5.9504
		0.6924	0.2975	29.7547	5.9509	
		0.6923	0.2975	29.7504	5.9501	
A2	0.5002	0.6925	0.2976	29.7590	5.9518	5.9512
		0.6924	0.2975	29.7547	5.9509	
		0.6924	0.2975	29.7547	5.9509	
A3	0.5106	0.6920	0.2974	29.7375	5.9475	5.9484
		0.6921	0.2974	29.7418	5.9484	
		0.6922	0.2975	29.7461	5.9492	
B1	0.5111	0.6923	0.2975	29.7504	5.9501	5.9501
		0.6923	0.2975	29.7504	5.9501	
		0.6923	0.2975	29.7504	5.9501	
B2	0.5102	0.6922	0.2975	29.7461	5.9492	5.9492
		0.6923	0.2975	29.7504	5.9501	
		0.6921	0.2974	29.7418	5.9484	
B3	0.5104	0.6918	0.2973	29.7289	5.9458	5.9466
		0.6920	0.2974	29.7375	5.9475	
		0.6919	0.2973	29.7332	5.9466	
C1	0.5103	0.3262	0.1402	35.0447	7.0089	7.0089
		0.3262	0.1402	35.0447	7.0089	
		0.3262	0.1402	35.0447	7.0089	
C2	0.5100	0.3261	0.1401	35.0340	7.0068	7.0083
		0.3262	0.1402	35.0458	7.0092	
		0.3262	0.1402	35.0447	7.0089	
C3	0.5101	0.3262	0.1402	35.0447	7.0089	7.0089
		0.3262	0.1402	35.0447	7.0089	
		0.3262	0.1402	35.0447	7.0089	

*A1-A3, B1-B3 and C1-C3 are three parallel samples of different three batches of FAAC.

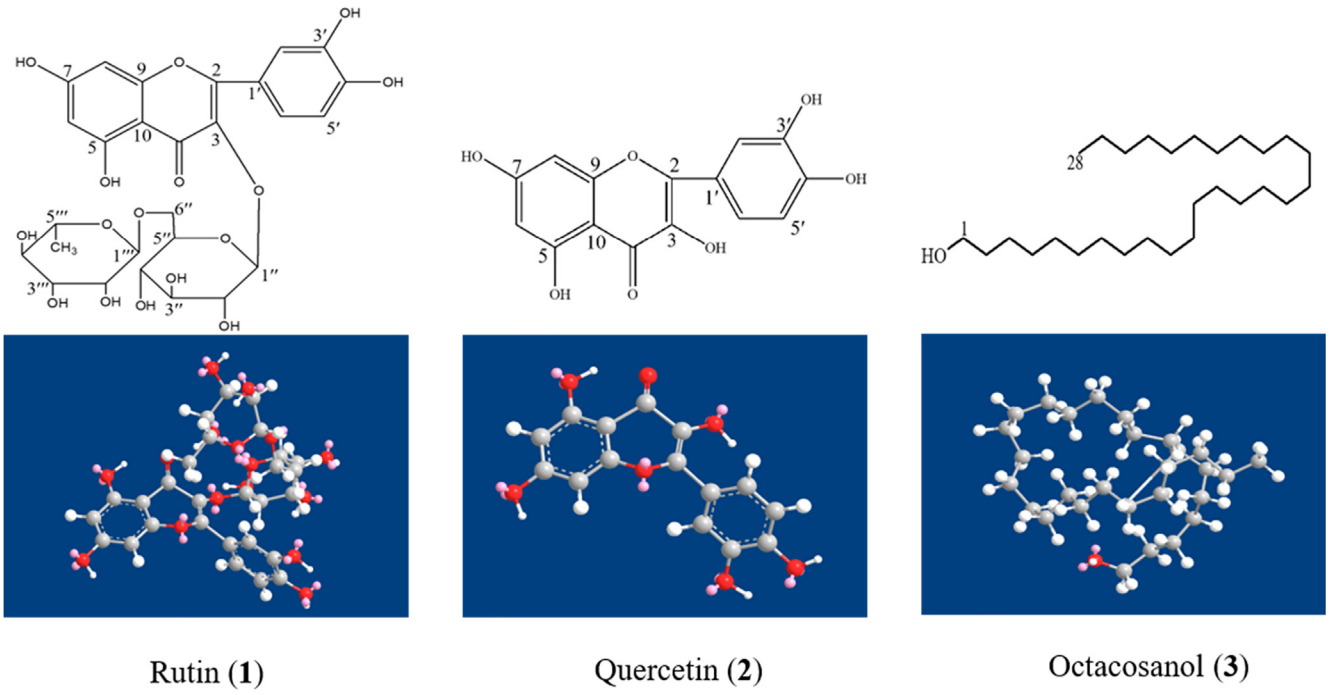

Fig. 1. Chemistry structures (2D and 3D) of compounds **1**–**3.**

(1H, d, *J* = 2.7 Hz, HO-2‴), 4.52 (1H, s, HO-3‴), 4.45 ~ 4.36 (1H, m, HO-4‴). ^{13}C NMR (150 MHz, DMSO d_6, TMS) 161.7 (C-5), 99.1 (C-6), 164.5 (C-7), 94.0 (C-8), 156.9 (C-9), 104.4 (C-10), 121.6 (C-1′), 116.7 (C-2′), 145.2 (C-3′), 148.9 (C-4′), 115.7 (C-5′), 122.1 (C-6′),157.1 (C-2),133.8 (C-3),177.8 (C-4), 101.6 (C-1″), 74.5 (C-2″), 76.9 (C-3″), 76.4 (C −4″), 70.4 (C-5″), 67.5 (C-6″), 101.2 (C-1‴), 71.0 (C-2‴), 70.8 (C-3‴), 72.3 (C-4‴), 68.7 (C-5‴), 18.2 (C-6‴).

Compound **2:** yellow green powder. ^{1}H NMR (600 MHz, DMSO d_6,TMS),δ_H: 9.58 (1H, s, OH-3), 12.50 (1H, s, OH-5), 6.21 (1H, d, *J* = 2.0 Hz, H-6), 10.76 (H, s, OH-7), 6.42 (1H, d, *J* = 2.0 Hz, H-8), 7.69 (1H, d, *J* = 2.2 Hz, H-2́), 9.35 (1H, s, OH-3́), 9.30 (1H, s, OH-4́), 6.90 (1H, d, *J* = 8.5 Hz, H-5́), 7.56 (1H, dd, *J* = 8.5 Hz, 2.2 Hz, H-6́); ^{13}C NMR (150 MHz, DMSO, TMS), δ_C: 148.1 (C-2), 136.2 (C-3), 176.3 (C-4), 161.2 (C-5), 98.6 (C-6), 164.9 (C-7), 93.8 (C-8), 156.6 (C-9), 103.5 (C-10), 120.4 (C-1́), 116.1 (C-2́), 145.5(C-3́), 147.2(C-4́), 115.5 (C-5́), 122.4 (C-6́). The data above were compared with those reported in the literature. So, compound **2** was identified as quercetin (Montserrat et al., 2012).

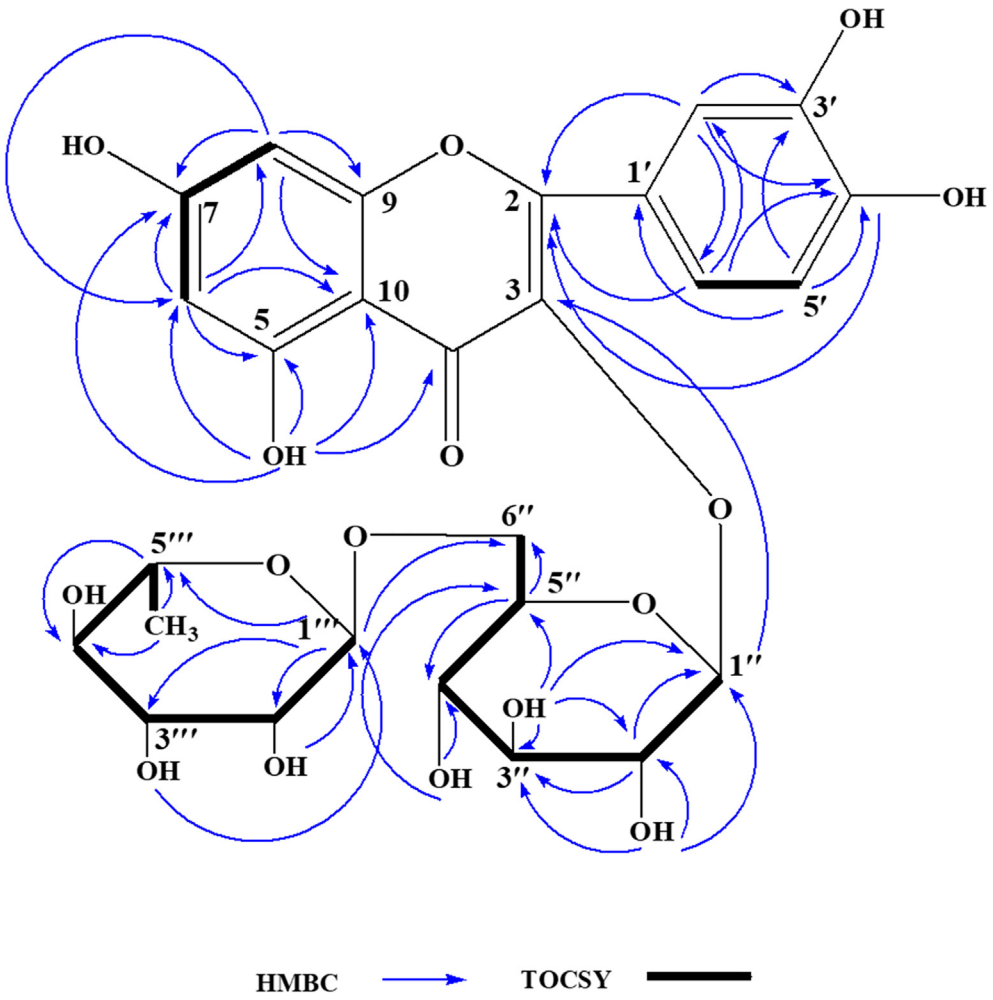

Fig. 2. The HMBC and TOCSY correlation spectra of compound **1.**

Compound **3:** white powder. LR-EIMS (*m*/*z*, 392), ^{1}H NMR (600 MHz, $CDCl_3$, TMS), δ_H: 3.59 (2H, t, *J* = 6.78 Hz, H-1), 2.02 (H, d, *J* = 5.16 Hz, OH-1), 1.52 (2H, m, H-2), 1.29 (50H, m, H-3 ∼ 27), 0.85 (3H, m, H-28). ^{13}C NMR (150 MHz, $CDCl_3$, TMS), δ_C: 63.1 (C-1), 32.8 (C-2), 31.9 (C-3), 29.7 (C4 ∼ 24), 27.1 (C-25), 25.7 (C-26), 22.7 (C-27), 14.1 (C-28). The data above were compared with those reported in the literature resulting in compound **3**, namely octacosanol (Amin et al., 2016).

3.2. Study on embryonic toxicity of zebrafish

3.2.1. Observation of development phenotype of zebrafish embryos

The methanol extract of FAAC induced a series of malformations during zebrafish embryonic development, including pericardial edema (Pe), yolk sac malformation (Ysd), eyes narrow, less melanin deposition, no exfoliation of the caudal ganglion and no shell-breaking, etc. See Fig. 3**.** Among them, Pe was the most apparent malformation (Fig. 3 **B3-B4, C2-C4**). Compared with the blank control group, the 1000 μg/mL administration group could cause embryos malformation after 24hpf (Fig. 3 **A-5**), and no obvious abnormality was found in other concentrations (Fig. 3 **A1-A4**). The embryos showed the eyes narrow, less melanin deposition, Pe and Ysd (Fig. 3 **B3 and B4**) at 250 and 500 μg/mL after 48 hpf, and the higher the administration concentration, the more significant the performance. After 72 hpf, the embryos showed the shorter body length and obvious Pe except for 62.5 μg/mL group. The 250 and 500 μg/mL groups showed Ysd, eyes narrow, less melanin deposition, no falling off of caudal segment and no shell-breaking (Fig. 3 **C2-C4**), and the higher the administration concentration, the more significant the toxicity.

3.2.2. Determination of spontaneous twitch, heart rate, and hatching rate of zebrafish embryos

There was no significant difference in the number of spontaneous twitch of embryos between the test groups (62.5 and 125 μg/mL) and the blank control group. However, there was a significant statistical difference for 500 μg/mL group. With the increase of concentration of the test groups, the number of spontaneous twitch of embryos increased in a concentration-dependent, but abnormal and almost zero at the high-dose 1000 μg/mL, which indicated that an excess high concentration would kill zebrafish embryos(Fig. 4 **A)** .

There were significant statistical differences on heart rate of zebrafish embryo between the test and the blank control groups except for those 62.5 and 125 μg/mL groups at 48hpf. With the increasing of concentration, the heart rate of zebrafish embryos slowed down in a concentration-dependent(Fig. 4 **B)** .

For the hatching rate of zebrafish embryos at 72 and 96 hpf, compared with the blank control group it showed significant differences except for the 62.5 μg/mL concentration group. The hatching rate decreased in a concentration dependent manner at 72 and 96 hpf with the increasing of concentration, and the zebrafish embryos were not out of the shell at 500 and 1000 μg/mL(Fig. 4 **C)** .

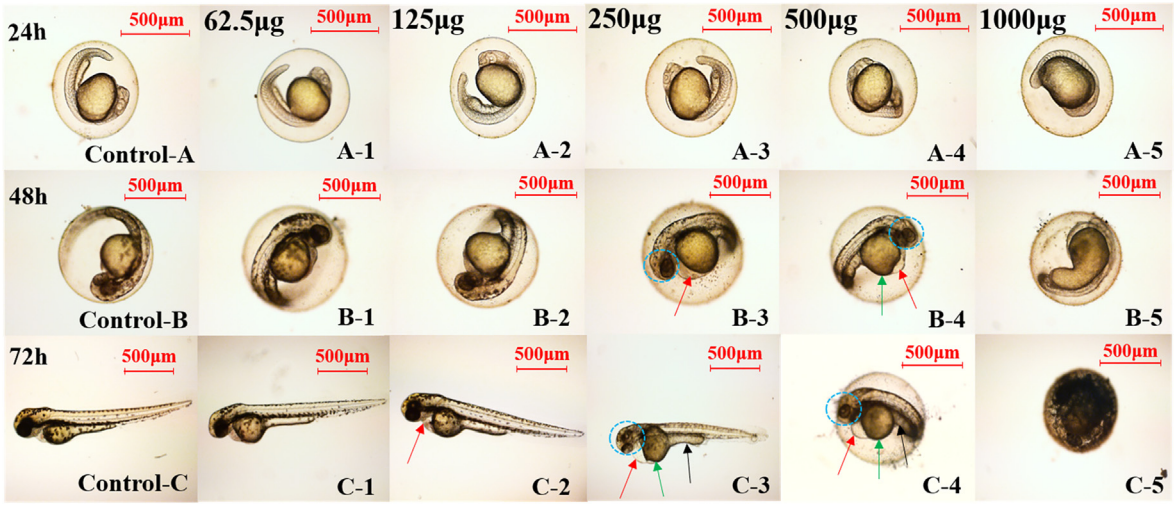

Fig. 3. Embryonic development phenotype of zebrafish at 24, 48 and 72 h in test groups. (A: Embryos were observed at 24 h after exposure. B: Embryos were observed at 48 h after exposure. C: Embryos were observed at 72 h after exposure.). Note: The red arrow indicates Pe; The green arrow indicates Ysd; The black arrow indicates that the tail section has not fallen off; The blue dotted line area indicates that the narrow eyes and less melanin.

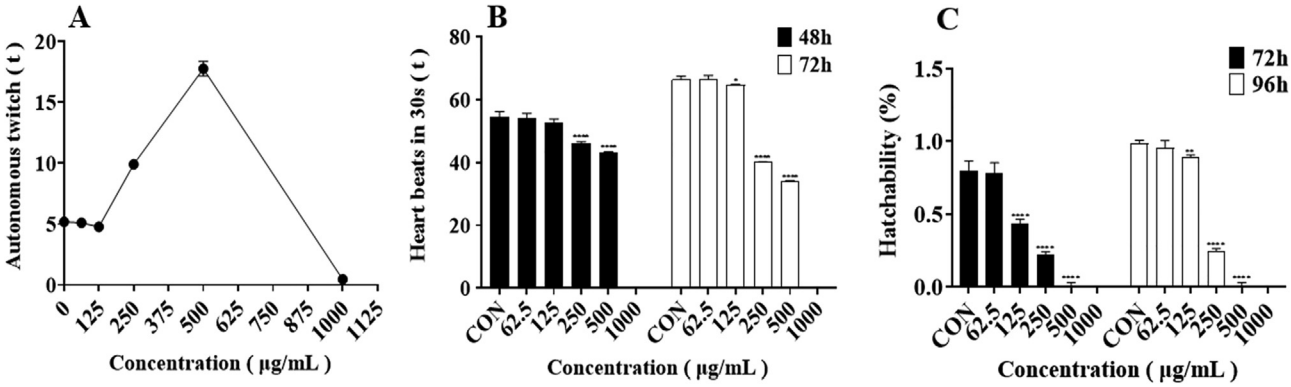

Fig. 4. The effect of FAAC on zebrafish embryonic development. (A: Number of spontaneous twitches of zebrafish embryos at 24hpf within 1 min. B: Heart beats of embryos in 30 s at each treatment time point. C: Hatchability at each observation time. Asterisk indicates that there is significant difference between the tests and the control. * $p < 0.05$; * * $p < 0.01$; * * * * $p < 0.0001$).

3.3. Study on the cardiotoxicity of zebrafish

3.3.1. Observation of heart development phenotype, SV-BA, and heart rate of the larvae

Paid attention to the indexes for evaluating whether the cardiac function was abnormal at each time point when observing the cardiotoxicity (Figs. 5 and 6). The blank control and 62.5 μg/mL group developed normally and the cardiovascular system was intact (Fig. 5 **A1-B1-C1**). In the 125, 250 and 500 μg/mL concentration groups, the larvae began to be found Pe, cardiac malformation, slow heart rate and SV-BA spacing increasing at 48th hour after administration. The abnormalities of various indexes of cardiac function became more obvious response to the increasing of administration time and dose.

3.3.2. Detection of cardiomyocyte apoptosis

Larvae were stained with AO and observed under a fluorescence microscope. See Fig. 7**.** The results revealed that no dense bright spots in the heart of larvae in the blank control group, which indicated there were no apoptotic cells. Compared with the blank control group except for 62.5 μg/mL, a large number of dense bright spots appeared in the heart of larvae, it indicated that the doses higher than 62.5 μg/mL could induce cardiomyocyte apoptosis.

3.4. Evaluation of intestinal hemostasis in zebrafish

3.4.1. LD_{50} test

The results of the six concentration gradients were shown in Fig. 8. Within the concentration range from 0 to 250 μg/mL, zebrafish did not die. The mortality of zebrafish was 5.0% for 500 μg/mL and 83.3% for 1000 μg/mL, up to 2000 μg/mL, the mortality was 100%. In the range of 500 ~ 2000 μg/mL, the zebrafish mortality showed a dose–effect with the sample concentration. The LD_{50} of methanol extract from FAAC was 770.6 μg/mL. The zebrafish mortality was 54.7% at the concentration of 770.6 μg/mL after verification, which accorded with the dose effect relationship. In subsequent experiments, the safe drug doses were selected as 0.3, 3.0, and 30.0 μg/mL.

3.4.2. Establishment of zebrafish bleeding model

The intestinal bleeding of zebrafish in each concentration group at 24th hour after administration of simvastatin (1.0, 2.0, 4.0, 6.0 and 8.0 μM) was shown in Fig. 9. Simvastatin at 1.0 μM did not cause intestinal bleeding (Fig. 8 **B**); Simvastatin at 2.0, 4.0, 6.0 and 8.0 μM led to zebrafish intestinal bleeding obviously in a concentration-dependent (Fig. 8 **C-F**). But zebrafish death occurred at simvastatin 4.0, 6.0 and 8.0 μM, and the mortality was dose-

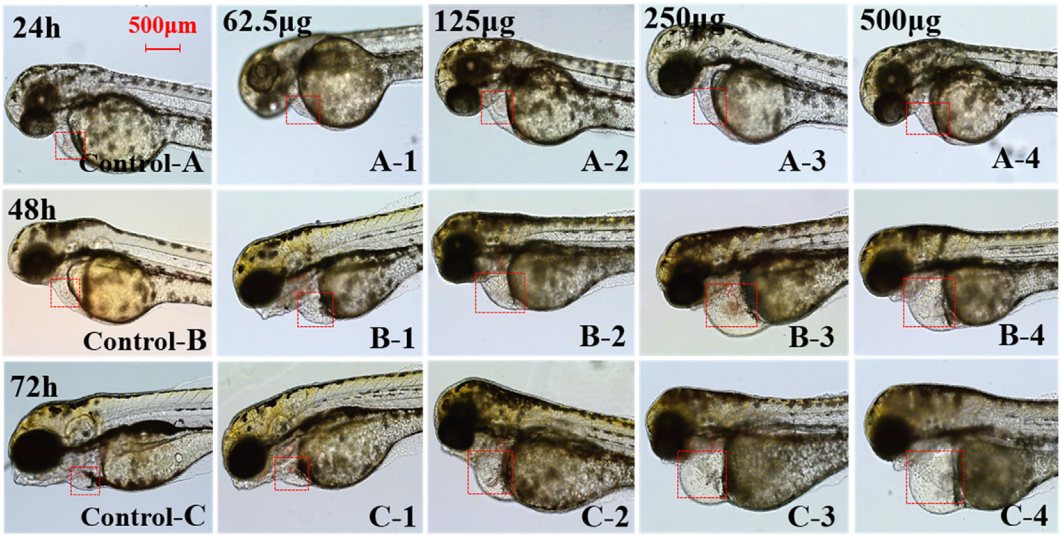

Fig. 5. Observation of cardiac developmental phenotype of zebrafish at 24, 48 and 72 h in test groups. (A: Larvae were observed at 24 h after exposure. B: Larvae were observed at 48 h after exposure. C: Larvae were observed at 72 h after exposure. The red area was the heart of zebrafish.).

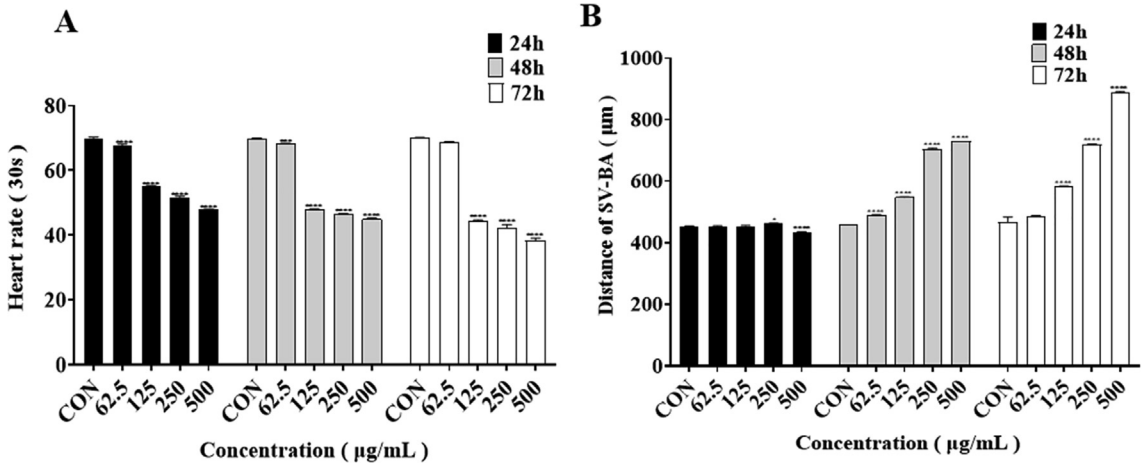

Fig. 6. The effect of the methanol extract of FAAC on heart development of zebrafish. (A: Heart beats of zebrafish in 30 s at each treatment time point. C: Distance of SV-BA at each observation time. Asterisk indicates that there is significant difference between the treatment and the control. * $p < 0.05$; * * * $p < 0.001$; * * * * $p < 0.0001$).

dependent (Fig. 9 **G**). Therefore, according to the modeling results, the simvastatin 4.0 μM was determined as the modeling dose concentration with large bleeding and low mortality.

3.4.3. Evaluation of intestinal bleeding rate

After administration of the methanol extract of FAA and FAAC in different concentration groups, the intestinal bleeding of zebrafish at 24th hour was shown in Fig. 10. There was no significant change in the bleeding phenomenon at a low concentration (0.3 μg/mL) for the two groups of FAA and FAAC (Fig. 10 **D1 E1**). The medium concentration (3.0 μg/mL) and high concentration (30.0 μg/mL) groups showed that the methanol extract of FAA and FAAC could significantly reduce intestinal bleeding of zebrafish, which indicated the FAA and FAAC had therapeutic effects on zebrafish intestinal bleeding at medium and high doses(Fig. 10 **D2-3 E2-3)** . But at the same concentration, methanol extract of FAAC had significantly higher hemostatic effect on zebrafish intestinal bleeding than AAF (Fig. 10 **B**). It showed that the hemostatic effect of FAAC was significantly enhanced after charcoal frying.

4. Discussion

In TCM theory, maintaining medicinal properties after the carbonisatus means that drugs can only be partially carbonized, let alone ashed, and the non carbonized part should still preserve the inherent properties of drugs. FAAC was processed from FAA at high temperature. The best processing temperature is 180 ℃ by using the double comprehensive evaluation of traditional characters and total flavonoids content (Lv et al., 2018). The processing of FAA aims to increase efficiency and reduce toxicity, which is to remove the toxicity of volatile oil components in FAA after processing (Lu et al., 2011). After charcoal frying, the insoluble calcium oxalate cluster crystal is significantly reduced, producing free calcium ions and increasing hemostasis, which is consistent with the TCM theory of charcoal frying hemostasis (Chen et al., 2019b). There is no relevant report on the chemical composition of FAAC up to date. In this study, the monomers were purified based on the determination of total flavonoids. Three compounds were isolated from FAAC and analyzed by comprehensive spectrum analysis. The complete structure of compound **1** (rutin) was assigned by 1D & 2D spectrum, especially the ten active hydrogens.

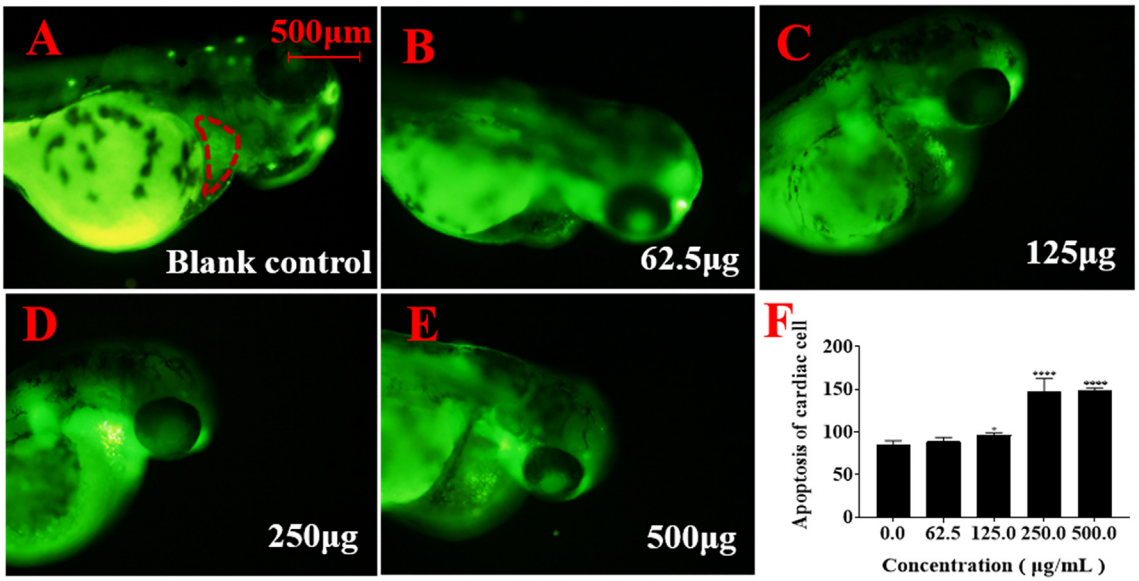

Fig. 7. The cardiomyocytes apoptosis of zebrafish induced by the methanol extract of FAAC. (A. The blank control; B. 62.5 μg; C. 125 μg; D. 250 μg; E. 500 μg; $^{*}p < 0.05$. $^{****}p < 0.0001$).

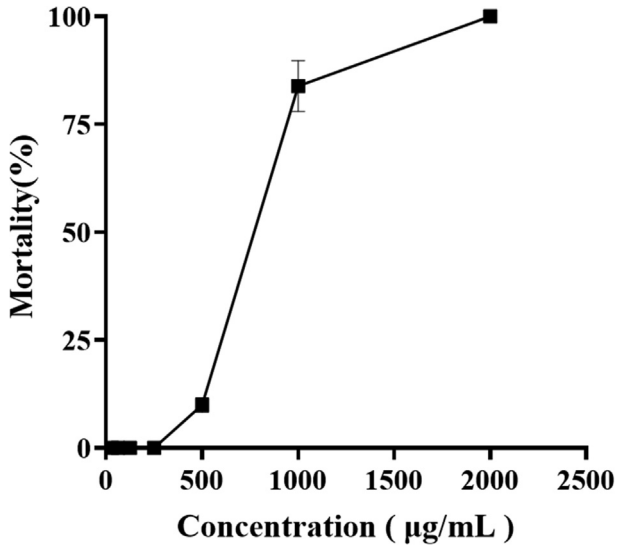

Fig. 8. Effect of the methanol extract of FAAC on mortality of zebrafish.

It improved the previous incomplete elucidation of rutin NMR data, and corrected the errors of some data. When analyzing ^{1}H–^{1}H COSY data, it was found that H-6 and H-8 in ring **A** were coupled with each other, however the correlation between H-6́ and H-2́ in ring **B** was not found. Therefore, the meta proton coupling relationship was not stable, even though on the large π bond formed by sp^2 hybrid orbit in the same aromatic ring. The ^{1}H–^{1}H COSY spectrum also revealed a more complex homonuclear hydrogen correlation. It was mainly the coupling relationship between the ten active hydrogen signals (four phenolic hydroxyl groups and six alcohol hydroxyl groups on the sugars), and the coupling between para aromatic hydrogen in the **B** ring. DMSO d_6 solvent as NMR reagent made the active protons be captured easily. At the same time, the resolution of 600 Hz high-resolution NMR spectrometer was much higher than that reported in the literature, which made some peak pattern more refined and the assessment more accurate. Comprehensively, this study also carried out a complete data assignment of quercetin, and corrected some errors in quercetin-relative literature.

Based on formulating the standard of FAAC by us (Jilin Province Code for Processing of Traditional Chinese Medicine, 2020 edition, China), in view of the fact that there are no reports on the toxicity of FAAC. Our team conducted zebrafish embryo and cardiac toxicity evaluation on the methanol extract of FAAC for the first time. The research results showed that the safe dosage was lower than 62.5 μg/mL. There was no obvious abnormality in the phenotypic development of zebrafish embryos until 24 h, but zebrafish had a strong autonomic twitch, which indicated that although the methanol extract of FAAC did not affect the morphological development of embryos, but could affect the normal development of an embryonic motor system or nervous system to some extent. For zebrafish at 48 and 72 h after fertilization, the methanol extract of FAAC showed obvious embryotoxicity, such as melanin reduction, body length shortening, Pe, tail node not falling off and other malformations. At the same time, it significantly reduced the hatching rate of zebrafish. Above 62.5 μg/mL the extract of FAAC could induce a series of embryonic malformations and show apparent toxic effects on the heart. The heart is the earliest organ that occurs and functions during zebrafish embryonic development (Cen et al., 2020). The heart of zebrafish basically develops and has a regular heartbeat 48 h after fertilization. The heart rate change is an important factor to evaluate cardiotoxicity (Duan et al., 2021). The pericardial region is widely used as a biomarker of zebrafish cardiotoxicity (Mitchell et al., 2019). Here the methanol extract of FAAC significantly reduced the heart rate of zebrafish embryos and larvae, and showed apparent Pe, an increase of SV-BA spacing and cardiomyocyte apoptosis. In addition, studies had shown that both rutin and quercetin had no developmental toxicity (Harwooda et al., 2007), and rutin could protect the heart by inhibiting oxidative stress (Ali et al., 2008). Therefore, it could be judged that rutin and quercetin were not responsible for the developmental and heart toxicity response to the methanol extract of FAAC in this study. The exact toxic components need to be further studied.

In addition, the zebrafish intestinal bleeding model was used to evaluate its hemostatic effect for the first time given the hemostatic effect of FAAC. Compared with the *in vitro* coagulation exper-

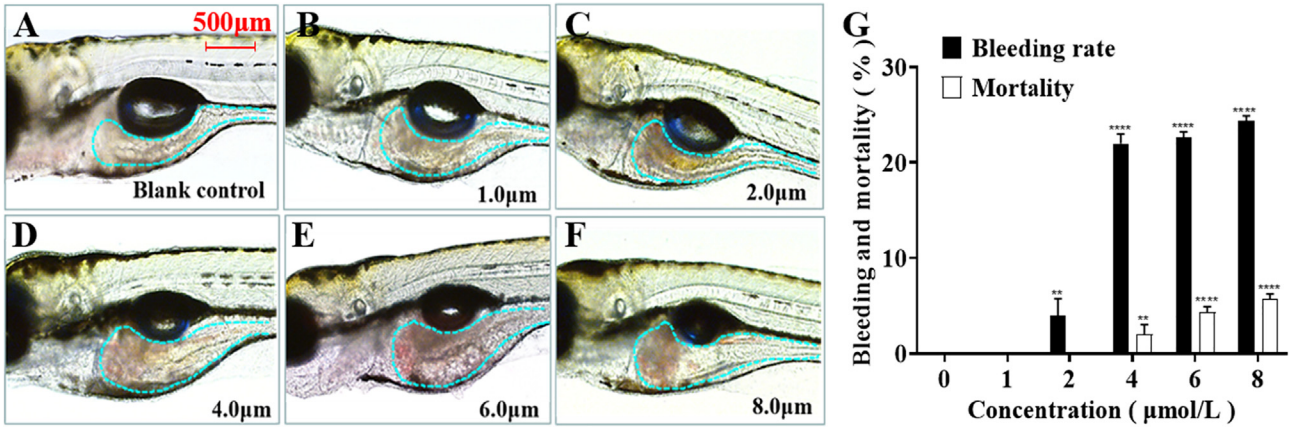

Fig. 9. Phenotype of intestinal bleeding in zebrafish induced by simvastatin. A: The blank control; B: 1.0 μM (bleeding rate: 0, mortality:0); C: 2.0 μM (13.3%, 0); D: 4.0 μM (73.3%, 7.3%); E: 6.0 μM (75.6%, 14.4%); F: 8.0 μM (81.1%, 18.9%); G: The bleeding rate and mortality of zebrafish. The bule area was the intestinal area * * $p < 0.01$; * * * $p < 0.001$; * * * * $p < 0.0001$).

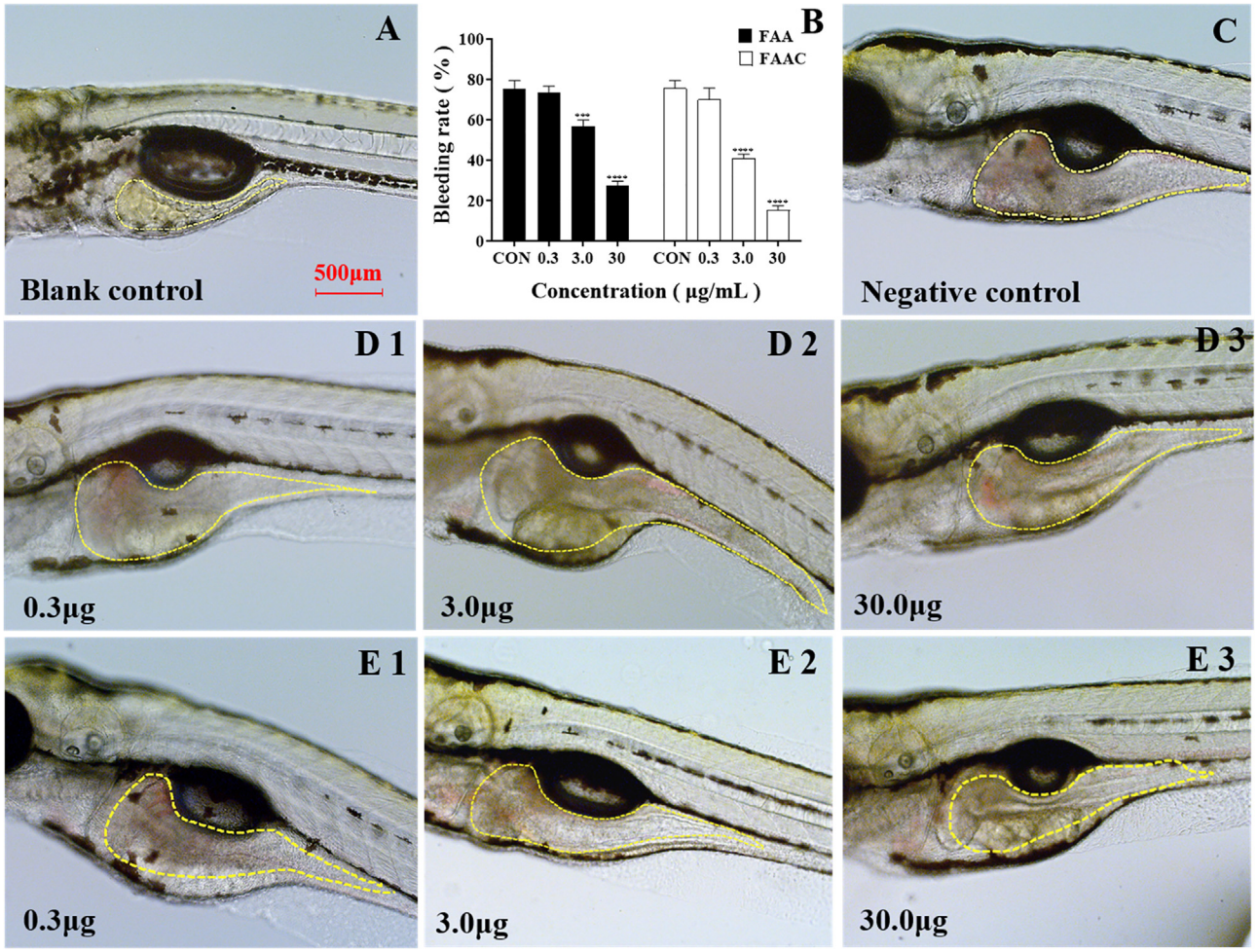

Fig. 10. Effects of FAA and FAAC test groups on intestinal bleeding in zebrafish. A: The blank control; B: The effects of FAA and FAAC on the bleeding rate of zebrafish. C: Negative control group (simvastatin 4.0 μM); D1-D3: FAA (bleeding rate: 73.3%, 56.0%, 27.8%); E1-E3: FAAC (bleeding rate: 70.1%, 41.1%, 15.6%). The yellow area was the intestinal. * * * $p < 0.001$; * * * * $p < 0.0001$.

iment of the mouse animal model, the zebrafish model is easier to observe the phenomenon of bleeding *in vivo*. It was difficult to observe intestinal bleeding in zebrafish induced by simvastatin. Therefore, hemoglobin was stained with *o*-anisidine to make the bleeding site more obvious. Although the administration dose of the methanol extract of FAAC was far less than LD_{50} and toxic dose, due to the simultaneous administration of simvastatin inducer and the methanol extract of FAAC, more attention should be paid to the death of zebrafish during the experiment. In the case of combined administration, the administration concentration is more practical

when the mortality was low or 0. The experimental results further verified that the hemostatic effect of FAA after charcoal frying was enhanced, which may be closely related to the formation of non-carbonized flavonoids or new substances. Modern pharmacological studies showed that flavonoids such as quercetin could aggregate platelets to produce a hemostatic effect (Chen et al., 2019; Janssen et al., 1998). Rutin had anti-inflammatory and antibacterial effects. It could reduce vascular permeability and brittleness to stop bleeding. At present, the combination of carboprost (Ca^{2+} carrier) and rutin could significantly inhibit adenylate cyclase by employing each action mechanisms (Kranc et al., 1992; Ippoliti et al., 1995) to promote smooth muscle contraction and reduce bleeding. Therefore, the enhancement cause of hemostasis attributed to rutin, quercetin or the synergistic effect of other chemical components in FAAC is still worthy of further study.

5. Conclusion

Herewith, this study further verified the theory of maintaining medicinal properties after the carbonisatus and provided a new idea and method for the related research of processing of Chinese materia medica. At the same time, for the first time the toxic effect of methanol extract of FAAC was evaluated, the zebrafish intestinal bleeding model was established to study the hemostatic effect of methanol extract before and after frying and charcoal of FAA, which laid a foundation for the clinical safety and scientific medication of FAAC.

Declaration of Competing Interest

The authors declare that they have no known competing financial interests or personal relationships that could have appeared to influence the work reported in this paper.

Acknowledgements

We are thankful for the support from the Project of Jilin Medical Products Administration, China (JMPA-2019-FAAC).
None.

Author contributions

LG conducted the experimental work and compiled the first draft the manuscript, XYW, XTS, ZYY, YLD, YL supervised, edited and prepared the final manuscript for submission. All authors read and approved the manuscript.

Appendix A. Supplementary material

Supplementary data to this article can be found online at https://doi.org/10.1016/j.jsps.2022.02.018.

References

Adrià, L.N., Wakako, I.O., Detmer, S., David, P., Charles, M.G., Maria, F., Geert, F.W., Sylvia, B., 2020. Feed, Microbiota, and Gut Immunity: Using the Zebrafish Model to Understand Fish Health. Frontiers in Immunology. 11, 114–128. https://doi.org/10.3389/fimmu.2020.00114.

Ali, M.S., Mudagal, M.P., Goli, D., 2008. Cardioprotective effect of tetrahydrocurcumin and rutin on lipid peroxides and antioxidants in experimentally induced myocardial infarction in rats. Pharmazie. 64 (2), 132–136. https://doi.org/10.1016/j.envpol.2021.117481.

Amin, E., Moawad, A., Hassan, H., 2016. Biologically-guided isolation of leishmanicidal secondary metabolites from Euphorbia peplus L. Saudi Pharmaceutical Journal. 25 (2), 236–240. https://doi.org/10.1016/j.jsps.2016.06.003.

Benchoula, K., Khatib, A., Jaffar, A., Ahmed, Q.U., Sulaiman, W.M.A.W., Wahab, R.A., El-Seedi, H.R., 2019. The promise of zebrafish as a model of metabolic syndrome. Exp. Anim. 68 (4), 407–416.

Cen, J., Jia, Z.-l., Zhu, C.-Y., Wang, X.-F., Zhang, F., Chen, W.-Y., Liu, K.-C., Li, S.-y., Zhang, Y., 2020. Particulate matter (PM10) induces cardiovascular developmental toxicity in zebrafish embryos and larvae via the ERS, Nrf2 and Wnt pathways. Chemosphere. 250, 126288. https://doi.org/10.1016/j.chemosphere.2020.126288.

Chen, L.L., Zhang, H.J., Chao, J., Liu, J.F., 2017a. Essential oil of Artemisia argyi suppresses inflammatory responses by inhibiting JAK/STATs activation. Journal of Ethnopharmacology. 204, 107–117. https://doi.org/10.1016/j.jep.2017.04.017.

Chen, Y., Chen, P.D., Bao, B.H., Shan, M.Q., Zhang, K.C., Cheng, F.F., Cao, Y.D., Zhang, L., Ding, A.W., 2017b. Anti-thrombotic and pro-angiogenic effects of Rubia cordifolia extract in zebrafish. Journal of ethnopharmacology. 219, 152–160. https://doi.org/10.1016/j.jep.2017.11.005.

Chen, Y.H., Chen, Q.W., Wang, X.Z., Sun, F., Fan, Y.W., Liu, X.R., Li, H.Y., Deng, Z.Y., 2019a. Hemostatic action of lotus leaf charcoal is probably due to transformation of flavonol aglycons from flavonol glucosides in traditional Chinses medicine. Journal of Ethnopharmacology 249,. https://doi.org/10.1016/j.jep.2019.112364 112364.

Chen, Z., Ye, S.Y., Yang, Y., Li, Z.Y., 2019b. A review on charred traditional Chinese herbs: carbonization to yield a hemostatic effect. Pharmaceutical Biology 57 (1), 498–506 https://doi:10.1080/13880209.2019.1645700.

Cui, Z.H., Huang, X.Z., Li, C., Li, Z., Li, M.J., Gu, L., Gao, L., Liu, D.H., Zhang, Z.Y., 2020. Morphology, Distribution, Density and Chemical Composition of Glandular Trichomes in Artemisia argyi (Asteraceae). International Journal of Agriculture & Biology., 1560–8530 https://doiorg/10.17957/IJAB/15.144.

Duan, M., Zhang, J., Liu, J., Qian, L.e., Chen, X., Zhao, F., Zhao, W., Zhong, Z., Yang, Y., Wang, C., 2021. Toxic effects of broflanilide exposure on development of zebrafish (Danio rerio) embryos and its potential cardiotoxicity mechanism. Environmental Pollution 286, 117481. https://doi.org/10.1016/j.envpol.2021.117481.

Elfawy, H.A., Anupriya, S., Mohanty, S., Patel, P., Ghosal, S., Panda, P.K., Das, B., Verma, S.K., Patnaik, S., 2021. Molecular toxicity of Benzo(a)pyrene mediated by elicited oxidative stress infer skeletal deformities and apoptosis in embryonic zebrafish. Science of The Total Environment. 789, 147989. https://doi.org/10.1016/j.scitotenv.2021.147989.

Guan, X., Ge, D.P., Li, S., Huang, K., Liu, J., Li, F., 2019. Chemical Composition and Antimicrobial Activities of Artemisia argyi Levl. et Vant Essential Oils Extracted by Simultaneous Distillation-Extraction, Subcritical Extraction and Hydrodistillation. Molecules. 24 (3), 483. https://doi.org/10.3390/molecules24030483.

Harwooda, M., Danielewska-Nikiela, B., Borzellecab, J.F., Flammc, G.W., Williamsd, G.M., Linese, T.C., 2007. A critical review of the data related to the safety of quercetin and lack of evidence of in vivo toxicity, including lack of genotoxic/carcinogenic properties. Food and Chemical Toxicology. 45 (2007), 2179–2205. https://doi.org/10.1016/j.fct.2007.05.015.

Ippoliti, C., Przepiorka, D., Mehra, R., Neumann, J., Wood, J., Claxton, D., Gajewski, J., Khouri, I., Van Besien, K., Andersson, B., Deisseroth, A.B., Dinney, C.P., 1995. Intravesicular carboprost for the treatment of hemorrhagic cystitis after marrow transplantation. Intravesicular carboprost for the treatment of hemorrhagic cystitis after marrow transplantation. 46 (6), 811–815.

Janssen, K., Mensink, R.P., Cox, F.J., Harryvan, J.L., Hovenier, R., Hollman, P.C., Katan, M.B., 1998. Effects of the flavonoids quercetin and apigenin on hemostasis in healthy volunteers: results from an in vitro and a dietary supplement study. The American Journal of Clinical Nutrition. 67 (2), 255–262. https://doi.org/10.1093/ajcn/67.2.255.

Administration, J.M.P., 2020. Jilin Province Code for Processing of Traditional Chinese Medicine. Jilin Science and Technology Press Co. Ltd, China, pp. 40–41.

Kang, C.P., Tu, H.C., Fu, T.F., Wu, J.M., Chu, P.H., Chang, D.T.H., 2018. An automatic method to calculate heart rate from zebrafish larval cardiac videos. BMC Bioinformatics. 19 (1), 169–178. https://doi.org/10.1186/s12859-018-2166-6.

Kong, H., Zhao, Y.S., Zhu, Y.F., Xiong, W., Luo, J., Cheng, J.J., Zhang, Y., Zhang, M.L., Qu, H.H., Zhao, Y., 2021. Carbon dots from Artemisiae Argyi Folium Carbonisata: strengthening the anti-frostbite ability. Artificial Cells, Nanomedicine, and Biotechnology 49 (1), 11–19 https://doi:10.1080/21691401.2020.1862134.

Kranc, D.M., Kim, J., Straus, F., Levine, L., 1992. Prophylactic and Therapeutic Carboprost Tromethamine Bladder Irrigation in Rats with Cyclophosphamide-Induced Hemorrhagic Cystitis. The Journal of Urology. 148 (4), 1326–1330. https://doi.org/10.1016/s0022-5347(17)36902-1.

Lee, D., Kim, C.E., Park, S.Y., Kim, K., Hiep, N., Lee, D., Jang, H.J., Lee, J., Kang, K., 2018. Protective Effect of Artemisia argyi and Its Flavonoid Constituents against Contrast-Induced Cytotoxicity by Iodixanol in LLC-PK1 Cells. International Journal of Molecular Sciences. 19 (5), 1387. https://doi.org/10.3390/ijms19051387.

Li, Y., 2021. Effect of compound rutin tablets combined with carboprost methyl ester suppository on postpartum hemorrhage. Henan Medical Research. 30 (04), 733–735.

Lu, J.H., Wu, C.R., Shi, Y., 2011. Toxicity of essential oil from Artemisia argyi against Oryzaephilus surinamensis (Linnaeus) (Coleoptera: Silvanidae). African Journal of Microbiology Research 5 (18), 2816–2819. https://doi.org/10.5897/AJMR11.179.

Lv, J.M., Li, X.N., Lin, H., Zhen, A.X., Wang, J.T., Wan, X.Y., Liu, J.W., Li, Y., Lin, Z., 2018. Study on Maintaing Medicinal Properties after the Carbonisatus Process of

Artemisiae Argyi Folium. World Latest Medicine Information (Electronic Version) 18 (10), 4–5 https://doi.org/10.19613/j.cnki.1671-3141.2018.10.002.
Makkar, H., Verma, S.K., Panda, P.K., Jha, E., Das, B., Mukherjee, K., Suar, M., 2018. In vivo molecular toxicity profile of dental bioceramics in embryonic Zebrafish (Danio rerio). Chemical Research in Toxicology. 31, 914–923 https://doi:10.1021/acs.chemrestox.8b00129.
Mitchell, C.A., Reddam, A., Dasgupta, S., Zhang, S., Stapleton, H.M., Volz, D.C., 2019. Diphenyl Phosphate-Induced Toxicity During Embryonic Development. Environ. Sci. Technol. 53 (7), 3908–3916.
Montserrat, D., Susana, G.M., Felipe, S.L., Ana, G.P., Celestino, S.B., 2012. Characterization of Sulfated Quercetin and Epicatechin Metabolites. Journal of Agricultural and Food Chemistry. 60 (14), 3592–3598. https://doi.org/10.1021/jf2050203.
Panida, Y., Suchada, S., Muenduen, P., 2020. Isolation, separation and purification of rutin from Banana leaves (Musa balbisiana). Industrial Crops and Products 149. https://doi.org/10.1016/j.indcrop.2020.112307.
Patel, P., Panda, P.K., Kumari, P., Singh, P.K., Nandi, A., Mallick, M.A., Das, B., Suar, M., Verma, S.K., 2020. Selective in vivo molecular and cellular biocompatibility of black peppercorns by piperine-protein intrinsic atomic interaction with elicited oxidative stress and apoptosis in zebrafish eleuthero embryos. Ecotoxicology and Environmental Safety. 192, https://doi:10.1016/j.ecoenv.2020.110321 110321.
Qian, L., Cui, F., Yang, Y., Liu, Y., Qi, S., Wang, C., 2018. Mechanisms of developmental toxicity in zebrafish embryos (Danio rerio) induced by boscalid. Science of the total environ. 634, 478–487. https://doi.org/10.1016/j.scitotenv.2018.04.012.
Seo, J.M., Kang, H.M., Son, K.H., Kim, J.H., Lee, C.W., Kim, H.M., Chang, S.I., Kwon, B. M., 2003. Antitumor Activity of Flavones Isolated from Artemisia argyi. Planta Medica. 69 (3), 218–222. https://doi.org/10.1055/s-2003-38486.
Sheel, R., Kumari, P., Panda, P.K., Jawed Ansari, M.D., Patel, P., Singh, S., Kumari, B., Sarkar, B., Mallick, M.A., Verma, S.K., 2020. Molecular intrinsic proximal interaction infer oxidative stress and apoptosis modulated inÂ vivo biocompatibility of P.niruri contrived antibacterial iron oxide nanoparticles with zebrafish. Environmental Pollution. 267, https://doi:10.1016/j.envpol.2020.115482 115482.
Song, X.W., Wen, X., He, J.W., Zhao, H., Li, S.M., Wang, M.Y., 2019. Phytochemical components and biological activities of Artemisia argyi. Journal of Functional Foods. 52, 648–662. https://doi.org/10.1016/j.jff.2018.11.029.
Verma, S.K., Panda, P.K., Kumari, P., Patel, P., Arunima, A., Jha, E., Husain, S., Prakash, R., Hergenröder, R., Mishra, Y.K., Ahuja, R., Varma, R.S., Suar, M., 2021a. Determining factors for the nano-biocompatibility of cobalt oxide nanoparticles: proximal discrepancy in intrinsic atomic interactions at differential vicinage. Green Chemistry. 23 (9), 3439–3458 https://doi:10.1039/d1gc00571e.
Verma, S.K., Nandi, A., Sinha, A., Patel, P., Jha, E., Mohanty, S., Panda, P.K., Ahuja, R., Mishra, Y.K., Suar, M., 2021b. Zebrafish (Danio rerio) as an ecotoxicological model for Nanomaterial induced toxicity profiling. Precis. Nanomed. 4 (1), 750–781 https://doi.org/10.33218/001c.21978.
Wang, N., Wan, J.B., Li, M.Y., Wang, Y.T., 2008. Advances in studies on Panax notoginseng against atherosclerosis. Chinese Traditional and Herbal Drugs. 2008 (05), 787–790.
Xia, J.-X., Zhao, B.-B., Zan, J.-F., Wang, P., Chen, L.-L., 2019. Simultaneous determination of phenolic acids and flavonoids in Artemisiae Argyi Folium by HPLC-MS/MS and discovery of antioxidant ingredients based on relevance analysis. Journal of Pharmaceutical and Biomedical Analysis. 175, 112734. https://doi.org/10.1016/j.jpba.2019.06.031.
Xiao, J.Q., Liu, W.Y., Sun, H.P., Li, W., Koike, K., Kikuchi, T., Yamada, T., Li, D.a., Feng, F., Zhang, J., 2019. Bioactivity-based analysis and chemical characterization of hypoglycemic and antioxidant components from Artemisia argyi. Bioorganic Chemistry. 92, 103268. https://doi.org/10.1016/j.bioorg.2019.103268.
Zhang, L.B., Lv, J.L., Chen, H.L., Yan, X.Q., Duan, J.A., 2013. Chemical constituents from Artemisia argyi and their chemotaxonomic significance. Biochemical Systematics and Ecology. 50, 455–458. https://doi.org/10.1016/j.bse.2013.06.010.
Zhang, L., Yan, Y.M., Wang, S.X., Ren, Z., Cheng, Y.X., 2019. Three new sesquiterpenoids with cytotoxic activity from Artemisia argyi. Natural Product Research. 35 (6), 893–899. https://doi.org/10.1080/14786419.2019.1610754.
Zhang, Q., Zhang, K.C., Lou, J.W., Guo, S.C., Zhang, Y., Yao, W.F., Tang, Y.P., Wu, J. H., Zhang, L., 2018. Simultaneous quantification of twelve compounds in ethyl acetate extracts of Euphorbia kansui before and after fry-baked with vinegar by UPLC–MS/MS and its toxic effect on zebrafish. Journal of Pharmaceutical and Biomedical Analysis. 155, 169–176. https://doi.org/10.1016/j.jpba.2018.03.035.
Zhu, L., Mu, X., Wang, K., Chai, T., Yang, Y., Qiu, L., Wang, C., 2015. Cyhalofop-butyl has the potential to induce developmental toxicity, oxidative stress and apoptosis in early life stage of zebrafish (Danio rerio). Environ. Pollut. 203, 40–49. https://doi.org/10.1016/j.envpol.2015.03.044.